Review Article

Childhood interstitial lung disease: A case-based review of the imaging findings

Markus Wu, Priya Girish Sharma, Dhanashree Abhijit Rajderkar

Department of Radiology, University of Florida College of Medicine, Gainesville, Florida, USA

Address for correspondence:
Dr. Dhanashree Abhijit Rajderkar, Department of Radiology, University of Florida College of Medicine, PO Box 100374, Gainesville, FL 32610, USA.
E-mail: rajdda@radiology.ufl.edu

Submission: 02-07-2020
Accepted: 12-08-2020
Published: 14-01-2021

Abstract:

Childhood interstitial lung disease (chILD) consists of a large, heterogeneous group of individually rare disorders. chILD demonstrates major differences in disease etiology, natural history, and management when compared with the adult group. It occurs primarily secondary to an underlying developmental or genetic abnormality affecting the growth and maturity of the pediatric lung. They present with different clinical, radiologic, and pathologic features. In this pictorial review article, we will divide chILD into those more prevalent in infancy and those not specific to infancy. We will use a case based approach to discuss relevant imaging findings including modalities such as radiograph and computed tomography in a wide variety of pathologies.

Keywords:

Alveolar capillary dysplasia, childhood interstitial lung disease, chronic lung disease of prematurity, congenital surfactant deficiency disorders

Childhood interstitial lung disease (chILD) consists of a large, heterogeneous group of individually rare disorders. The reported prevalence ranges from 0.13 cases/100,000 children younger than 17 years to 16.2 cases/100,000 children younger than 15 years.[1-3] ChILD demonstrates major differences in disease etiology, natural history, and management when compared with the adult group. ChILD occurs primarily secondary to an underlying developmental or genetic abnormality affecting the growth and maturity of the pediatric lung.[4] Therefore, a separate classification for chILD has been developed and updated most recently in 2013 by the chILD Research Network and recommended in the official American Thoracic Society clinical practice guideline on classification, evaluation, and management of chILD in infancy.[5]

In accordance with the "Image Gently" campaign launched by the Society for Pediatric Radiology, pediatric chest computed tomography (CT) examinations at our institution are performed with a low-dose protocol employing lower kVp, and automatic mA modulation with 1 mm × 1 mm lung algorithm reconstruction. In the appropriate patient population and indications, high-resolution chest CT including inspiratory and expiratory phases are obtained.

In this pictorial review article, we will divide chILD into those more prevalent in infancy and those not specific to infancy. We will use a case-based approach to discuss relevant imaging findings including modalities such as radiograph and CT in a wide variety of pathologies that are encountered but are rare.

Childhood interstitial lung disease entities more prevalent in infancy

Alveolar capillary dysplasia

Alveolar capillary dysplasia with misalignment of the pulmonary

Access this article online

Quick Response Code:

Website: www.thoracicmedicine.org

DOI: 10.4103/atm.ATM_384_20

How to cite this article: Wu M, Sharma PG, Rajderkar DA. Childhood interstitial lung disease: A case-based review of the imaging findings. Ann Thorac Med 2021;16:64-72.

veins (ACD-MPV) is a diffuse development disorder characterized by deficient alveolar capillaries, prominent right-to-left intrapulmonary vascular shunt, malpositioning of the pulmonary veins adjacent to the pulmonary arteries within the bronchovascular bundles, pulmonary lymphangiectasia, as well as muscular hypertrophy of the intralobular pulmonary arterioles, and resultant maldevelopment of the pulmonary lobules.[6] In addition, ACD-MPV is often associated with cardiovascular, gastrointestinal, or genitourinary system anomalies.[7] Genetic mutations and deletions within the Forkhead box transcription factor gene cluster on 16q24.1 have been reported in up to 40% of infants with ACD-MPV.[8,9] Imaging features include progressive ground-glass opacification, with occasional pneumothorax or pneumomediastinum secondary to air leaks. Interlobular septal thickening and peribronchovascular thickening can be seen in associated lymphangiectasia [Figure 1].[1,10] Diagnosis requires biopsy and genetic testing. It is near universally fatal secondary to progressive respiratory failure if lung transplantation is not performed in time.[11]

Pulmonary hypoplasia

Pulmonary hypoplasia is one of the alveolar growth abnormalities in which the bronchus and rudimentary lungs are present, while small airways, alveoli, and pulmonary vessels are decreased in size and number. It can be a primary phenomenon with intrinsic abnormal lung development, which is rare. Secondary pulmonary hypoplasia is much more common with compromised lung development due to intrauterine limitations on the thoracic space.[10] The most common cause of secondary pulmonary hypoplasia is congenital diaphragmatic hernia with abdominal organs occupying the thoracic space[1] [Figure 2]. Additional causes of secondary pulmonary hypoplasia include severe oligohydramnios (secondary to cystic renal dysplasia, prolonged rupture of membranes, or other genitourinary and placental abnormalities) and thoracic skeletal dysplasia (such as thanatophoric dysplasia and Jeune syndrome)[12] [Figures 3 and 4]. Imaging features include low lung volumes, without evidence of ground-glass opacities or cysts. In addition, the associated causes of secondary pulmonary hypoplasia usually can be found.[13]

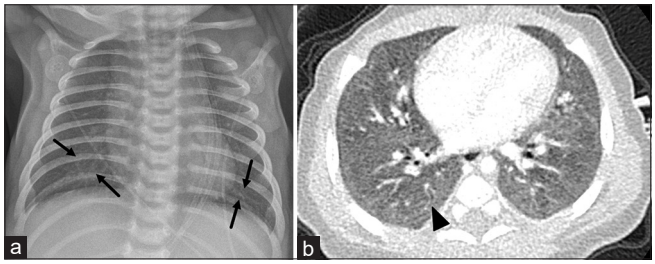

Figure 1: A 15-day-old term infant with respiratory distress, pathologically proven to have alveolar capillary dysplasia by bronchoscopy and tissue sample. (a) Chest radiograph shows a background of diffuse granular opacifications with peribronchial wall thickening (black arrows). (b) Axial chest computed tomography image better demonstrates diffuse ground-glass opacifications with peribronchial wall thickening (arrowhead)

Chronic lung disease of prematurity

Chronic lung disease of prematurity is classically described in premature infants exposed to prolonged high-pressure mechanical ventilation and high concentrations of oxygen, resulting in airway smooth muscle hypertrophy, epithelial squamous metaplasia, peribronchial fibrosis, and hypertensive vascular changes.[14] Imaging findings include impaired lung aeration, bronchial wall thickening, coarse reticular pulmonary opacities, and cystic lucencies, with a combination of alveolar septal fibrosis, atelectasis, and hyperinflated lung, resulting in variable lung volumes.[15,16] Oftentimes chest radiographs are sufficient to make the diagnosis [Figure 5]. However, CT is a better modality to better characterize the disease, assess for complications, and perform preoperative/pretransplant assessment[17] [Figure 6].

There is a "new" type of chronic lung disease of prematurity seen in extremely premature (24–26 weeks gestation) infants given the improved ventilatory technique and survival.[18] These patients will have received prenatal corticosteroids and have been ventilated for shorter periods with new ventilator settings,[13] resulting in milder imaging abnormalities with less airway and vascular disease, and less fibrosis [Figure 7]. Histologically, this is seen as arrested lung development corresponding to the gestation of the infant at delivery.[19]

Trisomy 21-related interstitial lung disease

Trisomy 21 (Down syndrome) is one of the lung growth disorders associated with chromosomal abnormalities. These patients were found to have

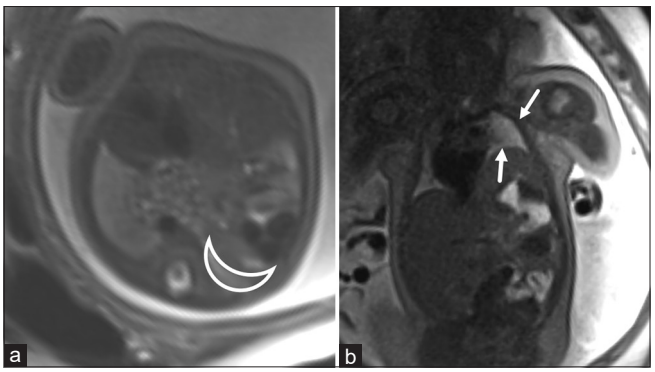

Figure 2: (a) Axial T2 image from fetal magnetic resonance imaging demonstrates a hypoplastic right lung (white crescent outline) in the setting of a right congenital diaphragmatic hernia. (b) Coronal T2 Image from fetal magnetic resonance imaging in a different patient shows a left congenital diaphragmatic hernia with a hypoplastic left lung (white arrows)

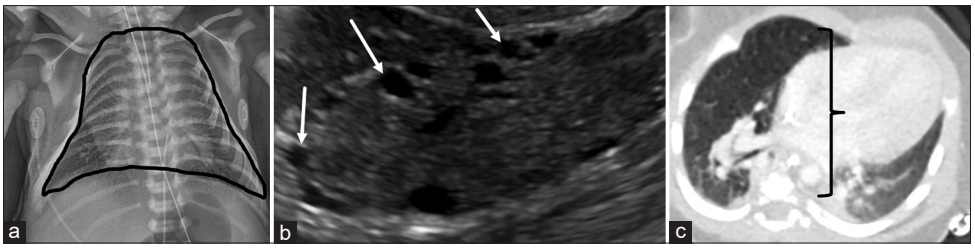

Figure 3: A 2-day-old male infant with cystic renal dysplasia presents with shortness of breath. (a) Chest radiograph shows hypoplastic lungs and a bell-shaped thorax (black outline). (b) Ultrasound of the right kidney in the sagittal view shows increased cortical echogenicity with multiple cortical and parenchyma cysts (white arrows). The left kidney is similar in appearance (not shown). (c) Axial chest computed tomography image shows disordered lung growth and reduced chest circumference (black bracket)

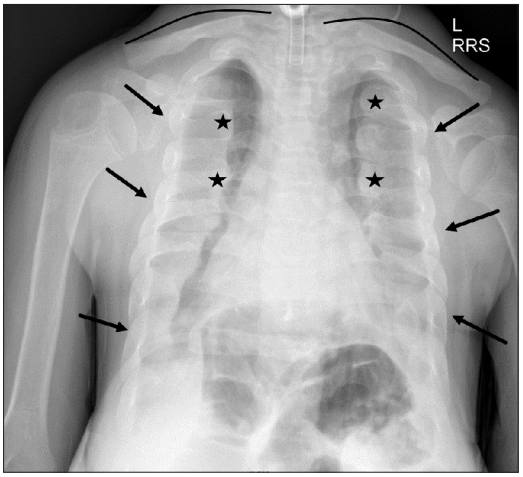

Figure 4: Chest radiograph of a 12-year-old male with Jeune Syndrome shows short rib dysplasia, bell-shaped narrow chest and hypoplastic lungs (black arrows), irregular costochondral junctions (black stars), and handlebar clavicles (black lines)

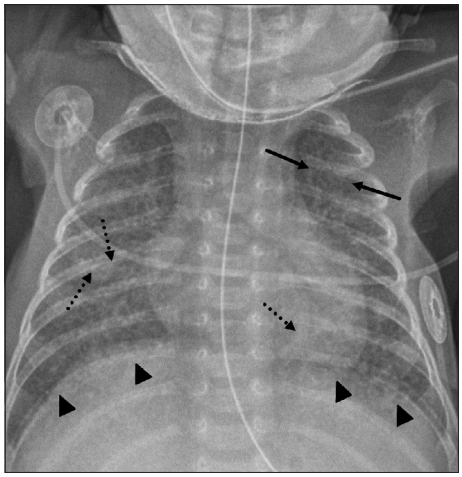

Figure 5: Chest radiograph of a 150-day-old female infant born at 32 weeks' gestation shows interstitial coarse thickening (black arrows), overinflation (black arrowheads), and bands of atelectasis (dashed black arrows), compatible with fibrosis in the setting of chronic lung disease of prematurity

decreased alveolar number and smaller alveolar surface area, as well as small peripheral subpleural cysts. On imaging, these cysts measure 1–2 mm in size and are subpleural along the lung periphery, fissures, and bronchovascular bundles[20,21] [Figure 8]. They have been reported to involve the anteromedial portion of the lungs.[20] Histologically, these cysts are enlarged subpleural airspaces in continuity with the proximal airways.[22] The etiology is unknown but thought to be related to pulmonary hypoplasia with Down syndrome.[23]

Congenital surfactant deficiency disorders

Surfactant deficiency disorders are caused by mutations in several genes, including genes for surfactant protein B, surfactant protein C, adenosine triphosphate–binding cassette transporter protein A3, thyroid transcription factor 1, and colony-stimulating factor 2 receptor (*CSF2RA* or *CSF2RB*).[5,24] Histologically, these genetic surfactant deficiency disorders are similar irrespective of the gene involved. Typical features include type 2 pneumocyte hyperplasia and varying degrees of intra-alveolar macrophages, proteinosis, or lipoproteinosis. On imaging, these patients present with low lung volumes and diffuse ground-glass opacities. Additional findings include cysts, and interlobular septal thickening with a crazy-paving pattern. Associated pectus excavatum has also been reported, which is hypothesized to be the sequelae of chronic restrictive lung disease in the developing chest wall [Figures 9-11].

Childhood Interstitial Lung Disease Entities Not Specific to Infancy

Noonan-related pulmonary lymphangiectasia

Noonan syndrome is an autosomal dominant congenital disease characterized by RASopathy (Ras/mitogen-activated protein kinase) mutation. It has similar clinical features to Turner syndrome.[25] Various abnormalities of the lymphatic system have been reported in patients with Noonan syndrome including intestinal lymphangiectasis, lymphedema, and pulmonary lymphangiectasia.[26,27] It is caused by dilation and proliferation of the lymphatic channels due to incompetent valves, or agenesis of the valves, with absence or interruption of the thoracic duct. Imaging findings include interlobular septal thickening, ground glass opacification, pleural effusions, or chylothorax [Figure 12].

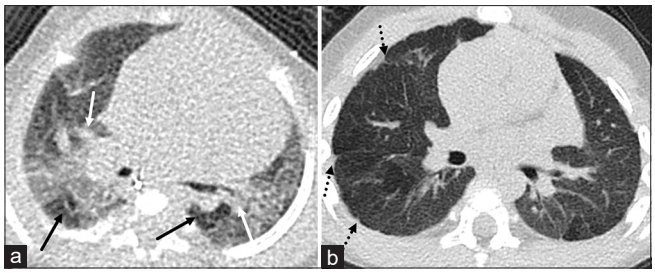

Figure 6: (a) Axial chest computed tomography image of a 5-month-old female infant born at 26 weeks' gestation shows diffuse ground-glass opacification with focal areas of air trapping (black arrows) and segmental atelectasis/scarring (white arrows). (b) Axial chest computed tomography image of a 3-year-old male born at 24 weeks' gestation shows subpleural reticulation (dashed black arrows) and scattered air trapping

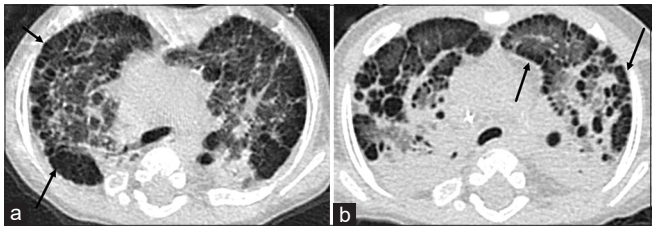

Figure 8: Two axial chest computed tomography images (a and b) in a 10-month-old male with trisomy 21 show extensive subpleural cysts (black arrows) peripherally and along the fissures and bronchovascular bundles

Blau syndrome – "pediatric sarcoidosis"

Blau syndrome classically presents in early childhood (under the age of 4 years) as a triad of granulomatous dermatitis, arthritis, and uveitis.[28] Recent studies have shown that Blau syndrome and early-onset sarcoidosis are the familial and sporadic forms, respectively, of the same disease.[29] Blau syndrome and early-onset sarcoidosis contrast with the adult-like form of sarcoidosis, which presents in older children and adolescents, clinically manifesting with systemic features of fever, weight loss, hilar adenopathy, and pulmonary infiltration.[30] Interstitial lung disease is a major feature in adults but not in children. Pulmonary involvement is rare and includes ground glass opacities in the both upper and lower lobes, adenopathy of axillary nodes, and bronchial granulomas [Figure 13].

Bronchiolitis obliterans

Bronchiolitis obliterans is a rare, fibrosing form of chronic obstructive lung disease that follows a severe insult to the lower respiratory tract and results in narrowing and complete obliteration of the small airways. Bronchiolitis obliterans in children is most often seen following a severe lower respiratory tract infection, most commonly adenovirus. It is also a known complication following lung transplantation, bone marrow, or hematopoietic stem cell transplantation. Microscopically, this corresponds to fibrosing inflammatory processes around the lumen of the bronchioles resulting in concentric narrowing and

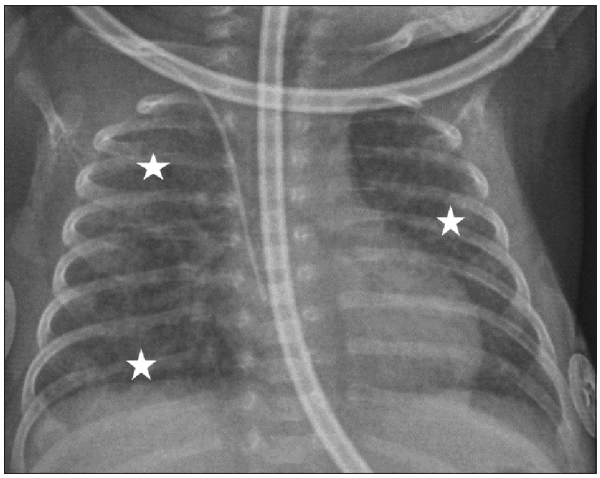

Figure 7: Chest radiograph of a 25-day-old female infant born at 25 weeks' gestation demonstrates scattered areas of atelectasis (white stars) compatible with the "new" type of chronic lung disease of prematurity with milder presentation

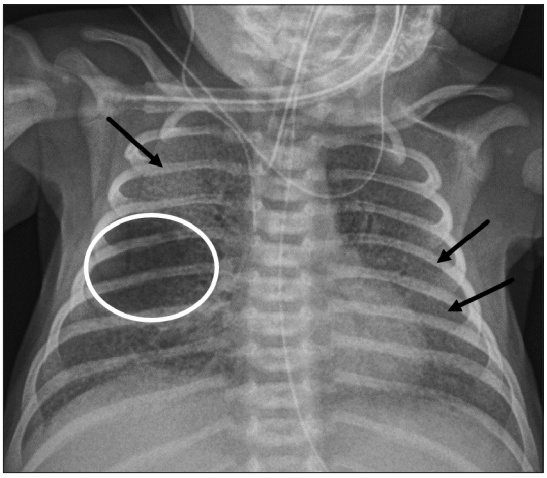

Figure 9: Chest radiograph of a term infant presenting with respiratory distress shows diffuse hazy airspace opacities (black arrows) and a pneumatocele (white outline). The patient was suspected to have a surfactant deficiency disorder and found to have adenosine triphosphate–binding cassette transporter protein A3 mutation

obliteration of small airways.[1] On imaging, bronchial wall thickening, ill-defined centrilobular nodular opacities, air trapping, and central bronchiectasis are common findings [Figure 14].

Organizing pneumonia

Organizing pneumonia (used to be described as bronchiolitis obliterans with organizing pneumonia) is histopathologically characterized by granulation tissues within small airways, alveolar ducts, and alveoli and by chronic inflammatory cell infiltration in alveolar walls.[31] When the cause is unknown, organizing pneumonia is classified as primary or cryptogenic. When a cause can be found, it is classified as secondary. Secondary causes include infection, drug reactions, collagen vascular disease, and after toxic-fume inhalation.[32] Common imaging findings include lower lung zone predominant

consolidation, patchy ground glass opacities in a subpleural or bronchovascular distribution, centrilobular nodules 3–5 mm in size, bronchial wall thickening and cylindrical bronchiectasis with air bronchograms, and pleural effusions[33] [Figure 15].

Adenovirus interstitial pneumonia

Adenovirus accounts for 5%–10% of acute respiratory infections in the pediatric population while it only accounts for <1% of respiratory illnesses in adults.[34] Adenovirus has its greatest effect in the terminal bronchioles and causes bronchiolitis and bronchiectasis.[35] The bronchiolitis may be necrotizing and result in a necrotizing bronchopneumonia. This is an increasing cause of morbidity and mortality in the immunocompromised pediatric population and has been documented in those who are post liver or kidney transplantation.[36] Swyer-James-MacLeod syndrome is considered to be an acquired disease secondary to adenovirus infection in childhood.[37] Imaging findings include patchy areas of consolidation in a segmental distribution with ground glass opacities [Figure 16], lobar collapse common in children, especially the right upper lobe[38] [Figure 17].

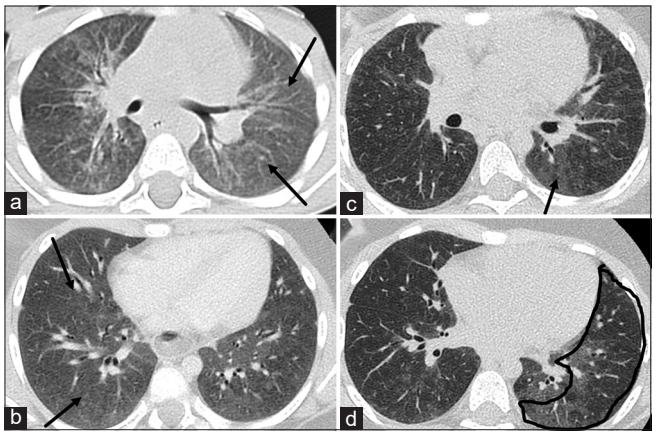

Figure 10: Serial axial computed tomography images through the mid lungs over a span of 7 years in a male with adenosine triphosphate–binding cassette transporter protein A3 mutation. a showed extensive ground glass opacities on the initial scan (black arrows). b performed two years later showed slightly improving ground glass opacities in the right lung (black arrows). c performed 5 years later showed continued improving ground glass opacity(black arrow). d performed 7 years later showed persistent air trapping and mosaic attenuation (black outline).

Chronic Eosinophilic Pneumonitis

Chronic eosinophilic pneumonitis is a rare pediatric respiratory disease[39] and characterized by a significant infiltration of the alveolar spaces and interstitium by eosinophils, with conservation of the normal lung structure. Respiratory symptoms usually last more than 2 weeks duration. The diagnosis is based on the demonstration of alveolar eosinophilia on bronchoalveolar lavage, and/or blood eosinophilia, with exclusion of other known causes of eosinophilia.[40] Pathology shows that exudate rich in eosinophils fills the lung interstitium and alveoli.[41] On imaging, peripheral nonsegmental pulmonary consolidations in mid to upper lung predominance are usually seen [Figure 18]. Chronic eosinophilic pneumonitis has an excellent response to steroids.

Pneumocystis Pneumonia

Pneumocystis pneumonia is caused by *Pneumocystis jiroveci* and most commonly occurs in immunocompromised children status post allogeneic hematopoietic stem cell transplantation, solid organ transplantation, or with congenital immunodeficiency syndromes and HIV. Subclinical infection is very common in immunocompetent children; two out of three children have antibodies by the age of 4 years.[42] Imaging features on CT include ground glass opacities, predominantly in the mid lung or perihilar region with peripheral sparing, and reticular opacities or interlobular septal thickening with crazy paving pattern [Figures 19 and 20]. Poorly ventilated zones are more prone to infection. Pneumatoceles can develop in 30% of cases. In patients treated with prophylactic medications, it can have an atypical appearance such as tree in bud nodules, lymphadenopathy, and pleural effusions.[43]

Chlamydia Pneumonia

Chlamydia pneumoniae is *a* common atypical respiratory

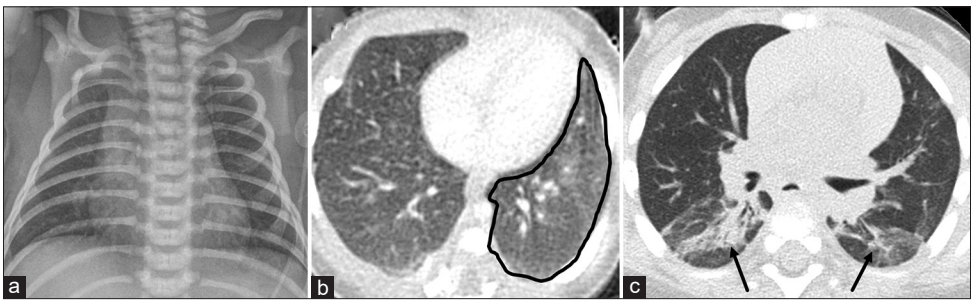

Figure 11: (a) Chest radiograph on day of life # 2 in a term infant experiencing desaturations shows nonspecific diffuse ground glass opacities. (b) Axial chest computed tomography image on day of life #9 demonstrates diffuse ground glass opacification (black outline). (c) Axial chest computed tomography image on day of life #270 shows bibasilar atelectasis and scarring (black arrows). This patient was found to have colony-stimulating factor 2 receptor B mutation

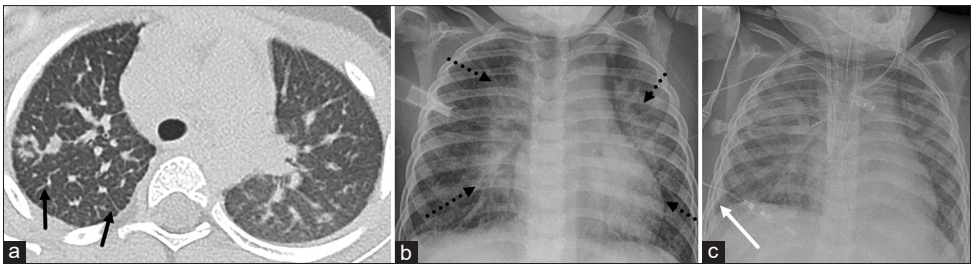

Figure 12: A 5-year-old male with Noonan syndrome. (a) Axial chest computed tomography image demonstrates interlobular septal thickening (black arrows) compatible with edema. (b) Next day chest radiograph shows worsening of perihilar predominant pulmonary edema (dashed black arrows). (c) Another chest radiograph performed hours later demonstrates worsening diffuse pulmonary edema, development of right-sided pleural effusion (white arrow) and interval placement of multiple lines and tubes including endotracheal tube

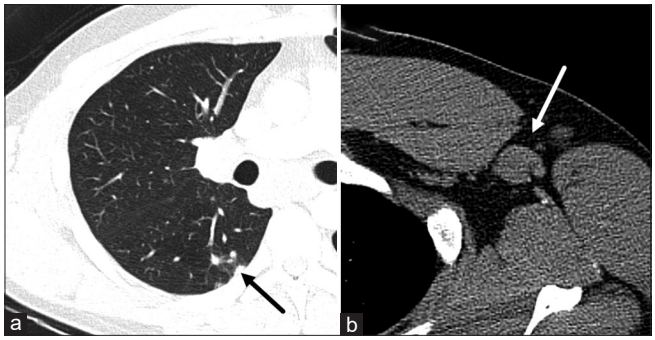

Figure 13: (a) Axial chest computed tomography image demonstrates "tree-in-bud" nodularity (black arrow) in this patient with pathologically proven Blau Syndrome. (b) Coned-down chest computed tomography in soft-tissue window of the same patient demonstrates left axillary adenopathy (white arrow)

Figure 14: Axial chest computed tomography image of an 8-year-old male with bronchiolitis obliterans after viral illness demonstrates bronchial wall thickening (black arrow) and scattered mosaic attenuation and air trapping (dashed black arrows)

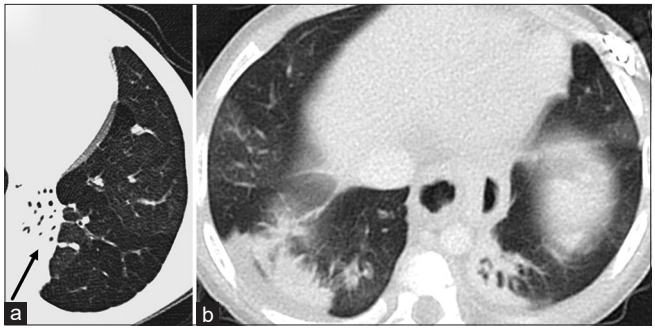

Figure 15: (a) Axial chest computed tomography image of a 10-year-old male with organizing pneumonia. Note the focal consolidation in the medial left lung base with bronchiectasis and air bronchograms (black arrow) and mild scattered air trapping. (b) Axial chest computed tomography image of a 2-year-old female with organizing pneumonia demonstrates the lower lung consolidations with right-sided pleural effusion

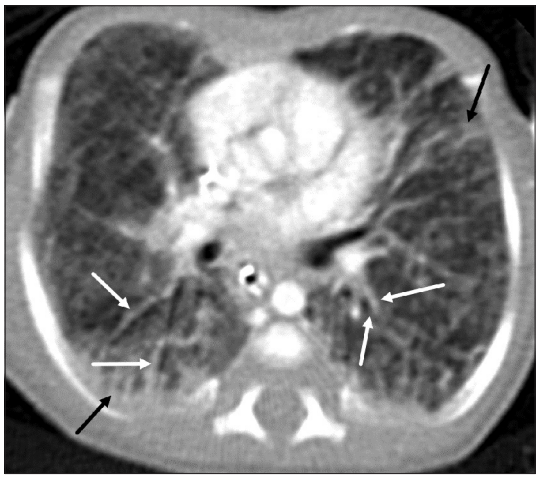

Figure 16: Axial chest computed tomography image of a 14-day-old infant with adenovirus infection shows diffuse ground glass opacification with superimposed peribronchial wall thickening (white arrows) with scatter subsegmental and bibasilar atelectasis (black arrows)

pathogen found in children 5–15-year-old with an incubation period of approximately 21 days.[44] It causes outbreaks in closed populations such as schools and coinfection with mycoplasma or streptococcus is common. Imaging appearance is variable. Airspace consolidation with or without centrilobular or peribronchovascular nodules is often seen and nonspecific. The presence of centrilobular or peribronchovascular nodules or bronchovascular bundle thickening without consolidation and with hyperexpansion or airway dilatation is more specific to *Chlamydia pneumoniae* pneumonia when compared to other atypical pneumonias[45] [Figure 21].

Vaping-Associated Lung Disease

Electronic cigarette or vaping product use-associated lung injury (EVALI) has become a serious public health

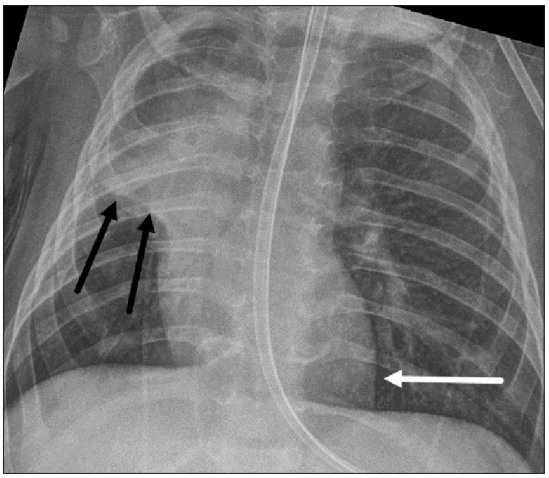

Figure 17: Chest radiograph of a 5-month-old male infant with adenovirus infection shows right upper lobe collapse (black arrows) and resultant rightward mediastinal shift (white arrow)

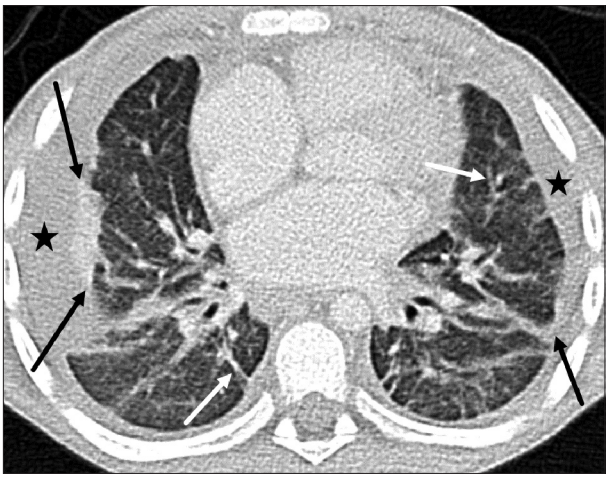

Figure 18: Axial chest computed tomography image of a 7-year-old male with chronic eosinophilic pneumonitis shows peripheral predominant airspace disease (black arrows) with interstitial thickening (white arrows) and pleural effusions (black stars)

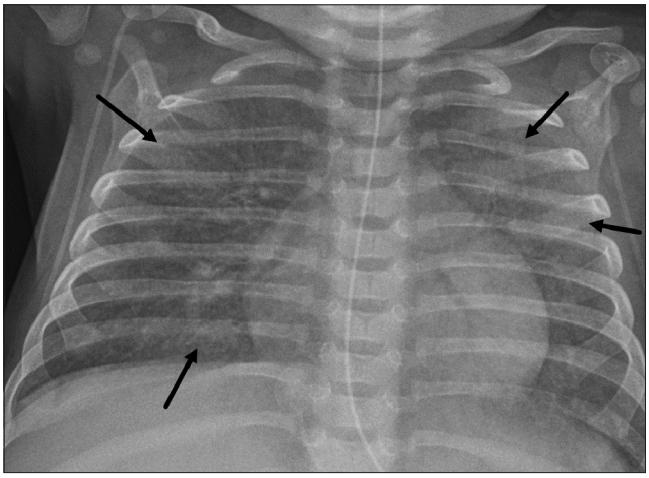

Figure 19: Chest radiograph of a 4-month-old HIV-positive male infant with pneumocystis pneumonia shows bilateral hazy airspace opacities (black arrows)

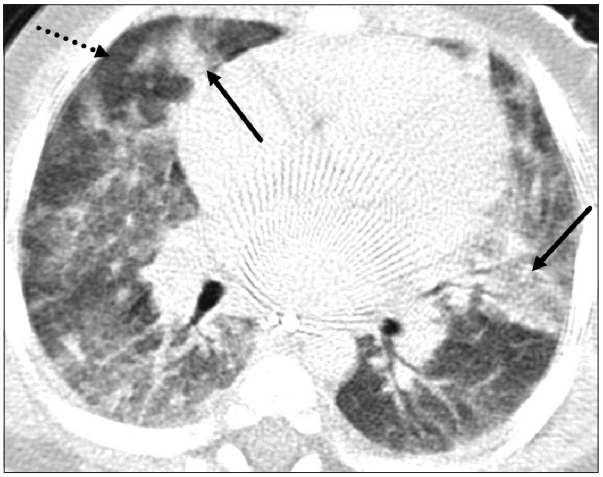

Figure 20: Axial chest computed tomography image of a 10-month-old male infant with pneumocystis pneumonia shows mid-lung predominant patchy airspace opacities (black arrows) with relative subpleural sparing (dashed black arrows)

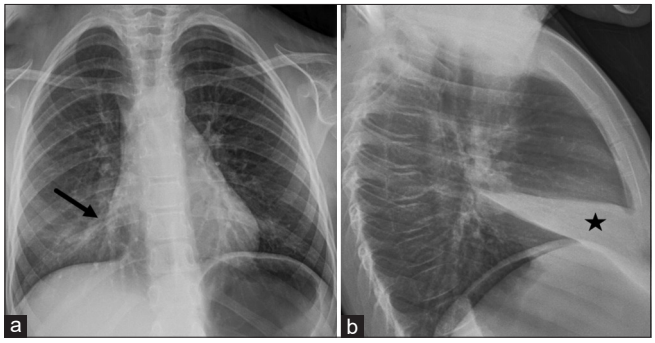

Figure 21: A 4-year-old female with chlamydia pneumonia. (a) Frontal chest radiograph shows lobar consolidation in the right middle lobe. Note how the right heart border is obscured on the frontal view (black arrow). (b) This corresponds to the consolidation in the right middle lobe on the lateral view (black star)

Figure 22: Axial chest computed tomography image of a 19-year-old male vaping marijuana shows diffuse perihilar ground glass opacification with peripheral sparing (black arrows) and peribronchovascular sparing (dashed black arrows)

problem with significant morbidity and mortality in young adults.[46] These patients present with respiratory symptoms such as dyspnea, as well as systemic symptoms including fever, myalgias, nausea/vomiting, and

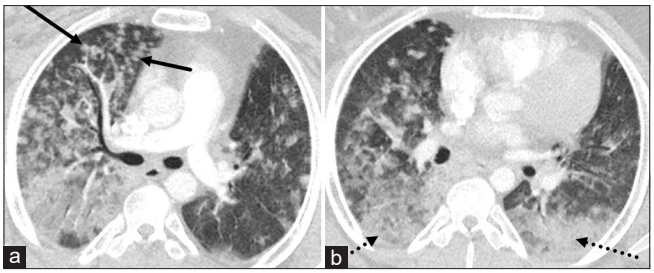

Figure 23: Axial chest computed tomography images (a and b) of a 17-year-old male with a history of vaping show a pattern consistent with diffuse alveolar damage with patchy nodular opacities in a centrilobular distribution (black arrows) and basilar consolidation (dashed black arrows)

fatigue. Bronchoalveolar lavage in these patients shows increased neutrophils and lipid-laden macrophages. Imaging plays a vital role in the initial detection and evaluation of progression of EVALI. There are several imaging patterns of EVALI in adults including diffuse alveolar damage, lipoid pneumonia, acute eosinophilic pneumonia, and organizing pneumonia.[47-49] In the adolescent population, the most common reported pattern is diffuse alveolar damage, which manifests as bilateral ground-glass opacities and consolidation with subpleural and lobular sparing, in a lower lobe predominance[50] [Figures 22 and 23]. The reversed halo sign (atoll sign) has been reported in pediatric patients with EVALI.[51]

Conclusion

chILDs encompass a large variety of both rare and more common pulmonary pathologies. Pathologies can be divided into two broad categories: Those associated or identified during infancy and those not specific to infancy. Genetic mutations play a large role in the pathogenesis and presentation of chILD and should be kept in mind. Knowledge of these pathologies allows for a multidisciplinary approach by pediatric radiologists, pulmonologists, and clinicians to provide appropriate and timely management.

Financial support and sponsorship
Nil.

Conflicts of interest
There are no conflicts of interest.

References

1. Semple TR, Ashworth MT, Owens CM. Interstitial lung disease in children made easier…well, almost. Radiographics 2017;37:1679-703.
2. Griese M, Haug M, Brasch F, Freihorst A, Lohse P, von Kries R, *et al*. Incidence and classification of pediatric diffuse parenchymal lung diseases in Germany. Orphanet J Rare Dis 2009;4:26.
3. Kornum JB, Christensen S, Grijota M, Pedersen L, Wogelius P, Beiderbeck A, *et al*. The incidence of interstitial lung disease 1995-2005: A Danish nationwide population-based study. BMC Pulm Med 2008;8:24.
4. Das S, Langston C, Fan LL. Interstitial lung disease in children. Curr Opin Pediatr 2011;23:325-31.
5. Kurland G, Deterding RR, Hagood JS, Young LR, Brody AS, Castile RG, *et al*. An official American Thoracic Society clinical practice guideline: Classification, evaluation, and management of childhood interstitial lung disease in infancy. Am J Respir Crit Care Med 2013;188:376-94.
6. Dishop MK. Diagnostic pathology of diffuse lung disease in children. Pediatr Allergy Immunol Pulmonol 2010;23:69-85.
7. Eulmesekian P, Cutz E, Parvez B, Bohn D, Adatia I. Alveolar capillary dysplasia: A six-year single center experience. J Perinat Med 2005;33:347-52.
8. Yu S, Shao L, Kilbride H, Zwick DL. Haploinsufficiencies of FOXF1 and FOXC2 genes associated with lethal alveolar capillary dysplasia and congenital heart disease. Am J Med Genet A 2010;152A: 1257-62.
9. Stankiewicz P, Sen P, Bhatt SS, Storer M, Xia Z, Bejjani BA, *et al*. Genomic and genic deletions of the FOX gene cluster on 16q24.1 and inactivating mutations of FOXF1 cause alveolar capillary dysplasia and other malformations. Am J Hum Genet 2009;84:780-91.
10. Lee EY. Interstitial lung disease in infants: New classification system, imaging technique, clinical presentation and imaging findings. Pediatr Radiol 2013;43:3-13.
11. Bishop NB, Stankiewicz P, Steinhorn RH. Alveolar capillary dysplasia. Am J Respir Crit Care Med 2011;184:172-9.
12. Biyyam DR, Chapman T, Ferguson MR, Deutsch G, Dighe MK. Congenital lung abnormalities: Embryologic features, prenatal diagnosis, and postnatal radiologic-pathologic correlation. Radiographics 2010;30:1721-38.
13. Liang T, Vargas SO, Lee EY. Childhood Interstitial (Diffuse) Lung Disease: Pattern Recognition Approach to Diagnosis in Infants. AJR Am J Roentgenol. 2019:1-10.
14. Bland RD, Coalson JJ, eds. Chronic lung disease in early infancy. Boca Raton, Fla: CRC Press, 1999.
15. Aukland SM, Halvorsen T, Fosse KR, Daltveit AK, Rosendahl K. High-resolution CT of the chest in children and young adults who were born prematurely: Findings in a population-based study. AJR Am J Roentgenol 2006;187:1012-8.
16. van Mastrigt E, Logie K, Ciet P, Reiss IK, Duijts L, Pijnenburg MW, *et al*. Lung CT imaging in patients with bronchopulmonary dysplasia: A systematic review. Pediatr Pulmonol 2016;51:975-86.
17. Tonson la Tour A, Spadola L, Sayegh Y, Combescure C, Pfister R, Argiroffo CB, *et al*. Chest CT in bronchopulmonary dysplasia: Clinical and radiological correlations. Pediatr Pulmonol 2013;48:693-8.
18. Northway WH Jr. Bronchopulmonary dysplasia: Twenty-five years later. Pediatrics 1992;89:969-73.
19. Jobe AJ. The new BPD: An arrest of lung development. Pediatr Res 1999;46:641-3.
20. Biko DM, Schwartz M, Anupindi SA, Altes TA. Subpleural lung cysts in Down syndrome: Prevalence and association with coexisting diagnoses. Pediatr Radiol 2008;38:280-4.
21. Joshi VV, Kasznica J, Ali Khan MA, Amato JJ, Levine OR. Cystic lung disease in Down's syndrome: A report of two cases. Pediatr Pathol 1986;5:79-86.
22. Gonzalez OR, Gomez IG, Recalde AL, Landing BH. Postnatal development of the cystic lung lesion of Down syndrome: Suggestion that the cause is reduced formation of peripheral air spaces. Pediatr Pathol 1991;11:623-33.
23. Cooney TP, Thurlbeck WM. Pulmonary hypoplasia in Down's syndrome. N Engl J Med 1982;307:1170-3.
24. Whitsett JA, Wert SE, Weaver TE. Diseases of pulmonary surfactant homeostasis. Annu Rev Pathol 2015;10:371-93.

25. Ford JJ, Trotter CW. Noonan Syndrome Complicated by Primary Pulmonary Lymphangiectasia. Neonatal Network 2015;34:117-25.
26. Hernandez RJ, Stern AM, Rosenthal A. Pulmonary lymphangiectasis in Noonan syndrome. AJR Am J Roentgenol 1980;134:75-80.
27. Noonan JA, Walters LR, Reeves JT. Congenital pulmonary lymphangiectasis. Am J Dis Child 1970;120:314-9.
28. Rose CD, Martin TM, Wouters CH. Blau syndrome revisited. Curr Opin Rheumatol 2011;23:411-8.
29. Rose CD. Blau syndrome: A systemic granulomatous disease of cutaneous onset and phenotypic complexity. Pediatr Dermatol 2017;34:216-8.
30. Becker ML, Martin TM, Doyle TM, Rosé CD. Interstitial pneumonitis in Blau syndrome with documented mutation in CARD15. Arthritis Rheum 2007;56:1292-4.
31. Lee JW, Lee KS, Lee HY, Chung MP, Yi CA, Kim TS, *et al*. Cryptogenic organizing pneumonia: Serial high-resolution CT findings in 22 patients. AJR Am J Roentgenol 2010;195:916-22.
32. Kligerman SJ, Franks TJ, Galvin JR. From the radiologic pathology archives: Organization and fibrosis as a response to lung injury in diffuse alveolar damage, organizing pneumonia, and acute fibrinous and organizing pneumonia. Radiographics 2013;33:1951-75.
33. Faria IM, Zanetti G, Barreto MM, Rodrigues RS, Araujo-Neto CA, Silva JL, *et al*. Organizing pneumonia: Chest HRCT findings. J Bras Pneumol 2015;41:231-7.
34. Franquet T. Imaging of pulmonary viral pneumonia. Radiology 2011;260:18-39.
35. Becroft DM. Bronchiolitis obliterans, bronchiectasis, and other sequelae of adenovirus type 21 infection in young children. J Clin Pathol 1971;24:72-82.
36. Chong S, Lee KS, Kim TS, Chung MJ, Chung MP, Han J. Adenovirus pneumonia in adults: Radiographic and high-resolution CT findings in five patients. AJR Am J Roentgenol 2006;186:1288-93.
37. Müller NL. Unilateral hyperlucent lung: MacLeod versus Swyer-James. Clin Radiol 2004;59:1048.
38. Chiu CY, Wong KS, Huang YC, Lin TY. Bronchiolitis obliterans in children: Clinical presentation, therapy and long-term follow-up. J Paediatr Child Health 2008;44:129-33.
39. Nathan N, Guillemot N, Aubertin G, Blanchon S, Chadelat K, Epaud R, *et al*. Chronic eosinophilic pneumonia in a 13-year-old child. Eur J Pediatr 2008;167:1203-7.
40. Marchand E, Cordier JF. Idiopathic chronic eosinophilic pneumonia. Orphanet J Rare Dis 2006;1:11.
41. Tassinari D, Di Silverio Carulli C, Visciotti F, Petrucci R. Chronic eosinophilic pneumonia: A paediatric case. BMJ Case Rep. 2013. p. 2013.
42. Pyrgos V, Shoham S, Roilides E, Walsh TJ. Pneumocystis pneumonia in children. Paediatr Respir Rev 2009;10:192-8.
43. Pitcher RD, Zar HJ. Radiographic features of paediatric pneumocystis pneumonia A historical perspective. Clin Radiol 2008;63:666-72.
44. Hammerschlag MR. Chlamydia trachomatis and Chlamydia pneumoniae infections in children and adolescents. Pediatr Rev 2004;25:43-51.
45. Nambu A, Saito A, Araki T, Ozawa K, Hiejima Y, Akao M, *et al*. Chlamydia pneumoniae: Comparison with findings of Mycoplasma pneumoniae and *Streptococcus pneumoniae* at thin-section CT. Radiology 2006;238:330-8.
46. Abbara S, Kay FU. Electronic cigarette or vaping-associated lung injury (EVALI): The tip of the iceberg. Radiol 2019;1:e190212.
47. Henry TS, Kanne JP, Kligerman SJ. Imaging of vaping-associated lung disease. N Engl J Med 2019;381:1486-7.
48. Sechrist JW, Kanne JP. Vaping-associated lung disease. Radiology 2020;294:18.
49. Henry TS, Kligerman SJ, Raptis CA, Mann H, Sechrist JW, Kanne JP. Imaging findings of vaping-associated lung injury. AJR Am J Roentgenol 2020;214:498-505.
50. Thakrar PD, Boyd KP, Swanson CP, Wideburg E, Kumbhar SS. E-cigarette, or vaping, product use-associated lung injury in adolescents: A review of imaging features. Pediatric Radiol 2020;50:338-44.
51. Artunduaga M, Rao D, Friedman J, Kwon JK, Pfeifer CM, Dettori A, *et al*. Pediatric chest radiographic and CT findings of lectronic cigarette or vaping product use-associated lung injury (EVALI). Radiology 2020;295:430-8.